PROCEEDINGS OF SCIENCE

Recent NA48/2 results on QCD and ChPT

Roberto Piandani[*†]
University and INFN of Pisa
E-mail: roberto.piandani@cern.ch

The NA48/2 experiment at CERN collected a very large sample of charged kaon decays into multiple final states. This data allow measurements related to QCD and Chiral Perturbation Theory (ChPT). In particular, we collected about 1500 events of the very rare decay $K^{\pm} \to \mu^{\pm} \nu e^{+} e^{-}$ over almost negligible background in the region with m($e^{+}e^{-}$) above 140 MeV, which is of great interest in ChPT, thanks to the m_{ee} spectrum and a model-independent measurement of the decay rate for this region. Also we performed the first observation of the rare decay $K^{+} \to \pi^{+}\pi^{0}e^{+}e^{-}$, with about 5000 candidates and 5% background contamination, and the preliminary branching ratio in the full kinematic region has been measured, in perfect agreement with theoretical predictions based on ChPT. Finally, we obtained our final measurement of the charged kaon semileptonic decays form factors based on 4.28 million $K^{\pm}e3$ and 2.91 million $K^{\pm}\mu 3$ selected decays, with the smallest uncertainty for $K^{\pm}e3$ and a competitive result for $K^{\pm}\mu 3$ and leading to the most precise combined $K^{\pm}l3$ result that reduces the form factor uncertainty of $|V_{us}|$.

XVII International Conference on Hadron Spectroscopy and Structure - Hadron2017
25-29 September, 2017
University of Salamanca, Salamanca, Spain

[*]Speaker.

[†]for the NA48/2 Collaboration: G. Anzivino, R. Arcidiacono, W. Baldini, S. Balev, J.R. Batley, M. Behler, S. Bifani, C. Biino, A. Bizzeti, B. Bloch-Devaux, G. Bocquet, N. Cabibbo, M. Calvetti, N. Cartiglia, A. Ceccucci, P. Cenci, C. Cerri, C. Cheshkov, J.B. Chèze, M. Clemencic, G. Collazuol, F. Costantini, A. Cotta Ramusino, D. Coward, D. Cundy, A. Dabrowski, P. Dalpiaz, C. Damiani, M. De Beer, J. Derré, H. Dibon, L. DiLella, N. Doble, K. Eppard, V. Falaleev, R. Fantechi, M. Fidecaro, L. Fiorini, M. Fiorini, T. Fonseca Martin, P.L. Frabetti, L. Gatignon, E. Gersabeck, A. Gianoli, S. Giudici, A. Gonidec, E. Goudzovski, S. Goy Lopez, M. Holder, P. Hristov, E. Iacopini, E. Imbergamo, M. Jeitler, G. Kalmus, V. Kekelidze, K. Kleinknecht, V. Kozhuharov, W. Kubischta, G. Lamanna, C. Lazzeroni, M. Lenti, L. Litov, D. Madigozhin, A. Maier, I. Mannelli, F. Marchetto, G. Marel, M. Markytan, P. Marouelli, M. Martini, L. Masetti, E. Mazzucato, A. Michetti, I. Mikulec, N. Molokanova, E. Monnier, U. Moosbrugger, C. Morales Morales, D.J. Munday, A. Nappi, G. Neuhofer, A. Norton, M. Patel, M. Pepe, A. Peters, F. Petrucci, M.C. Petrucci, B. Peyaud, M. Piccini, G. Pierazzini, I. Polenkevich, Yu. Potrebenikov, M. Raggi, B. Renk, P. Rubin, G. Ruggiero, M. Savrié, M. Scarpa, M. Shieh, M.W. Slater, M. Sozzi, S. Stoynev, E. Swallow, M. Szleper, M. Valdata-Nappi, B. Vallage, M. Velasco, M. Veltri, S. Venditti, M. Wache, H. Wahl, A. Walker, R. Wanke, L. Widhalm, A. Winhart, R. Winston, M.D. Wood, S.A. Wotton, A. Zinchenko, M. Ziolkowski.

PoS(Hadron2017)172

1. The NA48/2 Beam and Detector

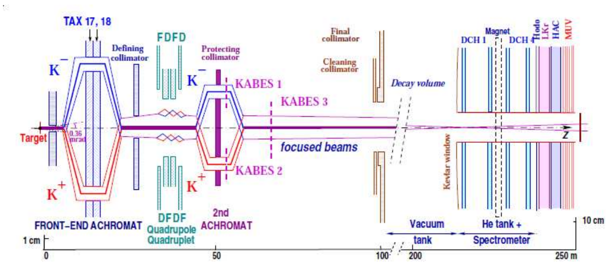

Figure 1: Schematic side view of the NA48/2 beam line, decay volume and detector.

Two simultaneous K^+ and K^- beams were produced by 400 GeV/c primary protons delivered by the CERN SPS. The layout of beams and detectors is shown in figure 1. The NA48/2 beam line was designed to select kaons with a momentum range of (60 ± 3) GeV/c. Both beams had a transverse size of about 1 cm. These beams were dominated by $\pi^\pm$, the $K^\pm$ component was about 6%. The beam kaons were delivered to a fiducial decay region of about 114 m long contained in a cylindrical vacuum tank.
The momenta of the charged decay products were measured in a magnetic spectrometer located downstream of the decay region. The spectrometer consisted of four drift chambers (DCH) and a dipole magnet between the second and third chambers, which provided a horizontal momentum kick of 120 GeV/c. The nominal spectrometer resolution was $\sigma_p/p = (1.0 + 0.044 \cdot p)\%$ where p is expressed in GeV/c. The spectrometer was followed by a plastic scintillator hodoscope (HOD), providing fast trigger signals and time measurement of charged particles with about 200 ps resolution for a single track. A 27 X_0 deep liquid Krypton electromagnetic calorimeter (LKr) located further downstream was used for charged particle identification and photon measurement. The LKr active volume of about 10 m^3 was segmented transversely into 13248 projective 2×2 cm^2 cells without any longitudinal segmentation. The energy resolution was $\sigma_E/E = 3.2\%/\sqrt{E} + 9\%/E + 0.42\%$, where E is in GeV. The identification of muons is performed with the MUon Veto system (MUV). It consists out of three planes of alternating horizontal and vertical scintillator strips. Each plane was shielded by a 80 cm thick iron wall. The time resolution of the system was below 1 ns. A detailed description of the whole setup can be found in [1].

2. The $K^\pm \to \mu^\pm \pi^0 \nu_\mu$ and $K^\pm \to e^\pm \pi^0 \nu_e$ form factors

The hadronic matrix element of semileptonic Kaon decays ($K^\pm l3$, $l = e, \mu$) is described by two dimensionless vector form factors $f_\pm(t)$, which depend on the squared four-momentum transferred to the lepton system, $t = (p_K - p_\pi)^2$. In the matrix element f_- is multiplied by the lepton mass and therefore its contribution can be neglected in $Ke3$ decays. In addition to the two vector form factors, also a scalar form factor exists (f_0). By construction $f_0(0) = f_+(0)$ and since $f_+(0)$ is not directly measurable it is customary to normalize to this quantity all the form factors so that:

$$\bar{f}_+(t) = \frac{f_+(t)}{f_+(0)} \quad \bar{f}_0(t) = \frac{f_0(t)}{f_+(0)} \quad \bar{f}_+(0) = \bar{f}_0(0) = 1.$$

There exist many parametrizations of the $Kl3$ form factors in the literature, a widely known and most used is the Taylor expansion:

$$\bar{f}_{+,0}(t) = 1 + \lambda^{'}_{+,0}\frac{t}{m^2_{\pi^\pm}} + \frac{1}{2}\lambda^{''}_{+,0}(\frac{t}{m^2_{\pi^\pm}})^2,$$

where $\lambda^{'}_{+,0}$ and $\lambda^{''}_{+,0}$ are the slope and the curvature of the form factors, respectively. A second parametrizations is present, this model, applying physical constraints, reduces to one the number of parameters used. A typical example is the pole one:

$$\bar{f}_{+,0}(t) = \frac{M^2_{V,S}}{M^2_{V,S} - t},$$

where the dominance of a single resonance is assumed and the corresponding pole mass $M_{V,S}$ is the only free parameter. A third parametrization exist, the Dispersive parametrization [2]

$$\bar{f}_+(t) = exp[(\Lambda_+ + H(t))t/m^2_\pi] \quad \bar{f}_0(t) = exp[(ln(C) - G(t))t/(m^2_K - m^2_\pi)]$$

2.1 Event selection and final background rejection

The data selection requires one charged track in the DCHs and a time coincidence with at least two clusters in the electromagnetic calorimeter (the two γ from the π^0 decay). Other requirements applied to the charged track are: the geometrical acceptance of the detector, a good reconstructed decay vertex inside the decay region, a proper timing and different conditions in the momentum depending on the track type ($p > 5GeV/c$ for the electron, $p > 10GeV/c$ for the muon). The electron identification is performed asking $E/p > 0.9$, where E is the energy deposited in the LKr and p is the momentum measured in the spectrometer, and no signal in time in the MUV system. The muon identification is performed asking an associated hit in time in the MUV system and $E/p < 0.9$. The background contribution has been estimated using the NA48/2 Monte Carlo. For $Ke3$ the background from $K^\pm \to \pi^\pm\pi^0$ has a significant contribution. In order to remove this contribution from the final sample a cut in the $P_t(\nu) >= 0.03GeV/c$ of the event is applied, the final amount is less than 0.027%. For $K\mu3$ selection, essential background may come from $K^\pm \to \pi^\pm\pi^0$ decays with a following $\pi^\pm \to \mu^\pm\nu$. The final contamination is reduces to 0.0264% cutting in $m(\pi^\pm\pi^0)$ and $m(\mu^\pm\nu)$.

2.2 Preliminary form factors results

The final statistics of selected data is 4.28×10^6 events for $K^\pm e3$, and 2.91×10^6 events for $K^\pm\mu3$. To extract the form factors an events-weighting fit is performed in $5 \times 5MeV$ cells in the Dalitz plot of E_{π^0} vs E_l energies, computed in the kaon rest frame. Combining the $K\mu3$ and $Ke3$ samples the results for the parameters of the parametrization based on Taylor expansion are:

$$\lambda^{'}_+ = 23.55 \pm 0.75(stat) \pm 1.23(syst) \qquad \lambda^{''}_+ = 1.73 \pm 0.29(stat) \pm 0.41(syst)$$
$$\lambda^{'}_0 = 14.90 \pm 0.55(stat) \pm 0.80(syst)$$

For the pole parametrization the results are:

$$M_V = 894.3 \pm 3.2(stat) \pm 5.4(syst) \qquad M_S = 1185.5 \pm 16.6(stat) \pm 35.5(syst)$$

For the dispersive parametrization are:

$$\Lambda_+ = (22.76 \pm 0.18(stat) \pm 0.55(syst)) \times 10^{-3} \qquad ln|C| = (180.1 \pm 4.9(stat) \pm 11.1(syst)) \times 10^{-3}$$

3. First observation of the $K^{\pm} \to \pi^{\pm}\pi^0 e^+ e^-$ decay

The $K^{\pm} \to \pi^{\pm}\pi^0 e^+ e^-$ decay is similar to the process $K^{\pm} \to \pi^{\pm}\pi^0\gamma$ but in this case instead of a real photon we have a virtual one ($K^{\pm} \to \pi^{\pm}\pi^0\gamma^*$, $\gamma^* \to e^+e^-$). Two possible mechanisms can lead to this rare kaon decay mode: Inner Bremsstrahlung (IB), where the γ^* is emitted by one of the charged mesons and Direct Emission (DE), when γ^* is radiated off at the weak vertex of the intermediate state of the process. For this reason the decay amplitude consists of two terms: the dominant long-distance IB contribution (pure electric part) and the DE component (electric and magnetic parts) . As a result, the differential decay width is a sum of IB, DE and interference terms. Detailed study of the various contributions to the amplitude of the considered rare process and the implication of this in the ChPT has reported in [3] and [4].

3.1 Event selection

The signal is characterized by 3 charged tracks and 2 photons coming from the decay of the neutral pion. Two independent clusters without associated track in the LKr (γ-candidates), with energy more than 3 GeV and distance to the adjacent clusters greater than 10 cm are required to identify the two photons which reconstruct the nominal neutral pion mass within $\pm 15 MeV/c^2$. Only events with $\Sigma Q = \pm 1$ are selected. The track with opposite charge is assumed to be an electron or positron, the two tracks with the same charge are assumed to be associated an electron (positron) or a pion. At this point the invariant mass of the 3 tracks system plus the pion is evaluated in the two configurations and the event is selected if $|M(K^{\pm}) - M(K^{\pm}_{PDG})| < 45 MeV/c^2$. In figure 2 the $M(K^{\pm})$ is reported.

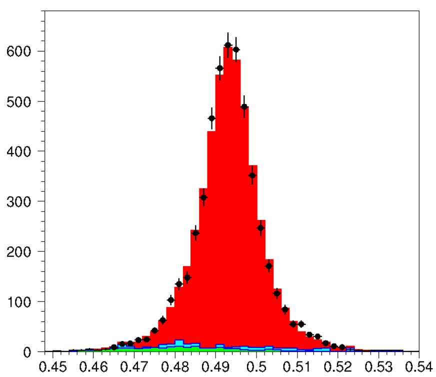

Figure 2: $M(\pi^{\pm}e^+e^-)$ invariant mass for data (black points), $K^{\pm} \to \pi^{\pm}\pi^0 e^+ e^-$ (red) and residual background (other colours).

3.2 Results

A sample of 5076 genuine $K^{\pm} \to \pi^{\pm}\pi^{0}e^{+}e^{-}$ events, with a residual background contamination $\sim 5.7\%$, has been collected by NA48/2 Collaboration. A preliminary result of the branching ratio is $Br(K^{\pm} \to \pi^{\pm}\pi^{0}e^{+}e^{-}) = (4.22 \pm 0.06(stat) \pm 0.04(syst) \pm 0.13(ext)) \times 10^{-6}$ where systematic errors include uncertainties on acceptance, particle identification, trigger efficiencies and radiative corrections (applied using PHOTOS in the MC sample). The dominant contribution to the error is the external one and it comes from the error in the $Br(\pi^{0}_{D})$. The result is in agreement with the ChPT prediction [4].

4. Study of the $K^{\pm} \to \mu^{\pm}\nu_{\mu}e^{+}e^{-}$ process

Radiative kaon decays can be used to test theories describing low energy Quantum Chromodynamics (QCD) such as Chiral Perturbation Theory (ChPT). The Standard Model can be tested using radiative decays in next-to-leading order in the chiral expansion without any further assumptions. The radiative leptonic process $K^{\pm} \to \mu^{\pm}\nu_{\mu}\gamma^{*}(\gamma \to e^{+}e^{-})$ can proceed via two different mechanisms: IB from the final state muon and DE of a virtual photon internally converted in a $e^{+}e^{-}$ pair. The phase space is dominated by IB and its contribution to the branching ratio can be calculated exactly. The interesting part of the phase space is the invariant mass of the $e^{+}e^{-}$ pair in the region $M_{ee} > 140 MeV/c^{2}$, where the ChPT form factors have an important contribution to the branching ratio. For this study a generator based on [5] with all form factors computed up to $O(p^{4})$ in ChPT has been used. Radiative corrections are included in the MC generation using the PHOTOS package.

4.1 Event selection

The $K^{\pm} \to \mu^{\pm}\nu_{\mu}e^{+}e^{-}$ selection is characterized by the presence of three charged tracks and a missing momentum carried away by the undetected neutrino. The three tracks have to form a good vertex inside fiducial decay region (98 m long) and to have a total charge of $|Q| = +1$. Each of the tracks has to pass through the geometrical acceptance of the Drift Chambers, HOD, LKr and MUV detector and to have momenta in the range between 3 and 50 GeV/c. The showers in the LKr produced by the charged tracks have to be isolated from each other by at least 20 cm. The total momentum of the three tracks has to be $p_{3track} < 66$ GeV/c in order to be consistent with the beam kaons. A cut is applied on the invariant mass of the $\mu - \nu$ system of $M_{\mu\nu} > 170 MeV/c^{2}$, to suppress events coming from $K^{\pm} \to \pi^{\pm}e^{+}e^{-}$ followed by a pion decay in muon. Electrons should leave all their energy in the LKr with an energy deposition shower shape different from the shape of showers produced by pions. To distinguish between genuine electrons and misidentified pions we require $0.95 < E/p < 1.05$ and use a linear discriminant variable, which makes use of the different shape and starting point of the created showers. For the cut E is the energy of the LKr cluster and p is the track momentum. The muon is required to leave only a small fraction of its energy in the LKr ($E/p < 0.2$) and to have a positive identification in the MUV detector. The signal acceptance is M_{ee} dependent and of the order of 12 - 15%.

4.2 Background and results

The remaining background is composed of decays with multiple pions in the final state misidentified as either muons or electrons. The background contamination coming from those modes can be studied directly in data using Wrong Sign (WS) selection. The WS selection is the same as the signal selection, but requiring two same-sign electrons/positrons and an opposite sign muon ($\mu^+e^-e^-$ or μe^+e^+). In the SM those modes (LFV) do not exist, therefore the only way to have such final state comes from processes constituting the background for the signal selection.
After the event selection, 1663 signal candidates are observed with an estimated background contamination of $54 \pm 10(stat) \pm 5(syst)$ events. The total number of kaons decayed in the fiducial volume is $(1.56 \pm 0.01) \times 10^{11}$. The z ($z = \frac{M_{ee}^2}{K_K^2}$) spectrum shown in figure 3 is compatible with the ChPT prediction. The branching ratio is computed for each of the z bins (15 bins in total). The results obtained in each bin are then summed to get the total branching ratio. The total model-independent branching ratio in the phase space $M_{ee} > 140MeV/c^2$ is $Br(K^\pm \to \mu^\pm \nu_\mu e^+ e^-) = (7.84 \pm 0.21(stat) \pm 0.08(syst) \pm 0.06(ext)) \times 10^8$. Radiative corrections have been included in the acceptance calculation using the PHOTOS package. The systematic uncertainty is 1.2 % and is dominated by the effect of radiative corrections on the signal acceptance and the background contamination.

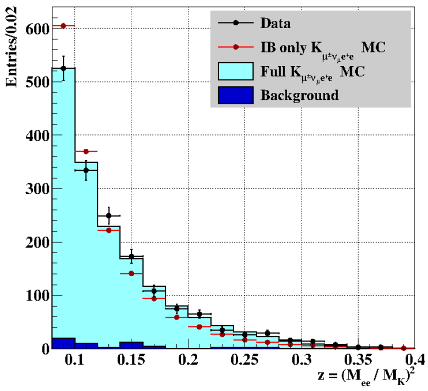

Figure 3: z distribution after the final selection. Data is presented with points with error bars. The estimated background is shown in dark blue. With brighter shaded histogram is presented the signal MC, scaled to the total number of expected events after background subtraction. The signal MC with only IB contribution is shown with points without error bars to demonstrate, that the shape predicted from ChPT is the one favoured by the data.

References

[1] V. Fanti *et al.*, [NA48 Collaboration], Nucl. Instrum. Meth. A **574** (2007) 433.

[2] V. Bernard, M. Oertel, E. Passemar, J. Stern, Phys. Rev. D80(2009) 034034.

[3] H. Pichl, Eur. Phys. J. C20 (2001) 371.

[4] L. Cappiello, O. Cata, G. O. D'Ambrosio, D. Gao, Eur. Phys. J C72 (2012) 1872.

[5] J. Bijnens, G. Ecker, J. Gasser , Nucl. Phys. B **396** 81-118 (1993).